

Time-resolved measurements of Cooper-pair radiative recombination in InAs quantum dots

S. S. Mou, H. Irie, Y. Asano, K. Akahane, H. Nakajima, H. Kumano, M. Sasaki, A. Murayama, and I. Suemune

Citation: *Journal of Applied Physics* **118**, 073102 (2015); doi: 10.1063/1.4928621

View online: <http://dx.doi.org/10.1063/1.4928621>

View Table of Contents: <http://scitation.aip.org/content/aip/journal/jap/118/7?ver=pdfcov>

Published by the [AIP Publishing](#)

Articles you may be interested in

[Temperature dependent and time-resolved photoluminescence studies of InAs self-assembled quantum dots with InGaAs strain reducing layer structure](#)

J. Appl. Phys. **106**, 013512 (2009); 10.1063/1.3159648

[Investigation of carrier dynamics on InAs quantum dots embedded in In Ga As/Ga As quantum wells based on time-resolved pump and probe differential photoluminescence](#)

Appl. Phys. Lett. **89**, 181924 (2006); 10.1063/1.2374801

[Time-resolved photoluminescence of InAs quantum dots in a GaAs quantum well](#)


Appl. Phys. Lett. **84**, 3046 (2004); 10.1063/1.1713052

[Time-resolved photoluminescence measurements of InAs self-assembled quantum dots grown on misorientated substrates](#)

Appl. Phys. Lett. **84**, 7 (2004); 10.1063/1.1637962

[Time-resolved probing of the Purcell effect for InAs quantum boxes in GaAs microdisks](#)

Appl. Phys. Lett. **78**, 2828 (2001); 10.1063/1.1370123




SHIMADZU Excellence in Science **Powerful, Multi-functional UV-Vis-NIR and FTIR Spectrophotometers**

Providing the utmost in sensitivity, accuracy and resolution for a wide array of applications in materials characterization and nanotechnology research

- Photovoltaics
- Polymers
- Thin films
- Paints/inks
- Ceramics
- FPDs
- Coatings
- Semiconductors

[Click here to learn more](#)



Time-resolved measurements of Cooper-pair radiative recombination in InAs quantum dots

S. S. Mou,¹ H. Irie (入江),² Y. Asano (浅野),³ K. Akahane (赤羽),⁴ H. Nakajima (中島),¹ H. Kumano (熊野),¹ M. Sasaki (佐々木),⁴ A. Murayama (村山),⁵ and I. Suemune (末宗)^{1,a)}

¹Research Institute for Electronic Science, Hokkaido University, Sapporo 001-0020, Japan

²NTT Basic Research Laboratories, NTT Corporation, Atsugi 243-0198, Japan

³Graduate School of Engineering, Hokkaido University, Sapporo 060-8628, Japan

⁴National Institute of Information and Communication Technology, Koganei 184-8795, Japan

⁵Graduate School of Information Science and Technology, Hokkaido University, Sapporo 060-0814, Japan

(Received 13 May 2015; accepted 3 August 2015; published online 17 August 2015)

We studied InAs quantum dots (QDs) where electron Cooper pairs penetrate from an adjacent niobium (Nb) superconductor with the proximity effect. With time-resolved luminescence measurements at the wavelength around 1550 nm, we observed luminescence enhancement and reduction of luminescence decay time constants at temperature below the superconducting critical temperature (T_C) of Nb. On the basis of these measurements, we propose a method to determine the contribution of Cooper-pair recombination in InAs QDs. We show that the luminescence enhancement measured below T_C is well explained with our theory including Cooper-pair recombination. © 2015 AIP Publishing LLC. [<http://dx.doi.org/10.1063/1.4928621>]

I. INTRODUCTION

Quantum-entangled photon pair (QEPP) sources play an important role in quantum information and communications technologies. Parametric down conversion (PDC) in an optical non-linear crystal has been widely used for sources to generate QEPPs.^{1,2} The pair generation rate of PDC has recently been dramatically improved, enabling an entanglement swapping at a telecom band at a practically sound rate.³ In the PDC, however, the emission of higher photon-number components is unavoidable, which should increase a risk of eavesdropping in the application to quantum key distribution. The PDC is not deterministic but probabilistic, which would complicate the synchronization between different device units in large-scale system integration.

The implementation of QEPP sources with solid-state devices has the potential for large-scale system integration as well as deterministic on-demand pair generation with nearly zero probabilities of higher photon-number components. Semiconductor quantum dots (QDs) are representative examples, where the electrons and holes recombine to emit a pair of photons. In the method by Fattal *et al.*,⁴ QEPPs were generated with the superposition of two sequentially emitted single photons with a time delay by passing them through short and long parallel paths to compensate the time delay and were measured in the post-selection. Biexciton-exciton cascaded photon-pair emission from QDs is another well known method, and the violation of Bell's inequality without any additional operations was demonstrated by using isotropic QDs grown with droplet epitaxy.⁵ Salter *et al.* demonstrated an entangled light-emitting diode (LED) which contains a QD and could emit QEPPs by electrical excitation.⁶ However, most of photon pairs emitted from QDs grown with a normal method fail to be QEPPs due to their

exciton-state fine structure splitting induced mainly by QD-shape anisotropy.⁷

We have proposed and have been working on a new method based on superconductors, where QEPPs can be generated through the radiative recombination of Cooper pairs.⁸ Electrons in superconductors form Cooper pairs which are spin-singlet entangled pairs.⁹ At a superconductor/normal-metal interface, Cooper pairs penetrate into the normal region by the proximity effect.¹⁰ We fabricated an InGaAs-based LED with a niobium (Nb) superconducting (SC) electrode for the *n*-type contact. We observed drastic enhancement of the LED output below the Nb SC critical temperature (T_C).¹¹ We analyzed luminescence of a Cooper pair with the second-order perturbation theory, where a Cooper pair recombines with a pair of holes.¹² The theory predicted luminescence enhancement below T_C . We demonstrated that the observed luminescence enhancement is well explained with the theory.¹³ We also observed sharp reduction of the LED luminescence decay time constant with another SC-LED below T_C , and also demonstrated a good agreement with our theory.^{14,15} With these results, we evidenced the active role of Cooper pairs in radiative recombination in SC-LEDs.

However, SC-LEDs demonstrated in the previous works have been based on quantum well (QW) active regions. Our first proposal of the on-demand QEPP generation was based on a QD.⁸ Cooper pairs are bosons and due to their coherent nature their number states are not fixed.¹⁵ While Cooper pairs penetrate from the SC electrode into the semiconductor region, it is minority holes injected from the counter *p*-type electrode that regulate the photon emission process. In this regard, we proposed to control the QEPP generation process by regulating the hole-number states via the valence-band lowest quantum state of a QD under the Pauli's exclusion principle.⁸

In this paper, we study luminescence of an InAs QD heterostructure doped *n*-type and in close proximity to a Nb superconductor with time-resolved measurements. We

^{a)}Electronic mail: isuemune@es.hokudai.ac.jp

demonstrate abrupt luminescence enhancement at temperature below T_C . We propose a method to determine the contribution of Cooper-pair recombination without ambiguity. We also study the measured temperature dependence of the Cooper-pair recombination with our theoretical model. Finally, we discuss the difference of the presently measured temperature dependence and the previously measured properties of SC-LEDs.

II. SAMPLE PREPARATION

In our previous SC-LEDs, active QW regions were at the center of p - n junction. Without external bias, p - n junctions induce internal built-in potential and deplete the active layers. For the purpose of time-resolved measurements under pulsed-laser excitation, we adopted n -type doping in an InAs QD heterostructure rather than the p - n junction. The sample was grown on a (311)B InP substrate with molecular-beam epitaxy (MBE). The growth was started with 50-nm-thick $\text{In}_{0.53}\text{Ga}_{0.47}\text{As}$ /100-nm-thick $\text{In}_{0.52}\text{Al}_{0.48}\text{As}$ layers for selective etching of the InP substrate. Then, the growth was followed by a heterostructure of 200-nm-thick n - $\text{In}_{0.53}\text{Ga}_{0.25}\text{Al}_{0.22}\text{As}$ /20-nm-thick n - $\text{In}_{0.53}\text{Ga}_{0.35}\text{Al}_{0.12}\text{As}$ /5-monolayer of InAs QDs/100-nm-thick n - $\text{In}_{0.53}\text{Ga}_{0.35}\text{Al}_{0.12}\text{As}$ /10-nm-thick n - $\text{In}_{0.53}\text{Ga}_{0.47}\text{As}$. The n -type doping level was $\sim 1 \times 10^{18} \text{ cm}^{-3}$. The most part of the heterostructure was grown at 470°C , but InAs QDs were grown at 530°C to reduce the QD density and it was $3.4 \times 10^{10} \text{ cm}^{-2}$.¹⁶ The average QD lateral size and height were 57 nm and 5.6 nm, respectively. The thin n - $\text{In}_{0.53}\text{Ga}_{0.47}\text{As}$ layer on top of the surface is for ohmic contact to a subsequently evaporated Nb layer.

The semiconductor wafer surface was etched into a periodic array of pillars with different diameters ranging from

200 nm to $2 \mu\text{m}$ with electron-beam lithography and the subsequent reactive ion etching (RIE). Inductively coupled plasma (ICP) was used for RIE and the pillars height was $\sim 900 \text{ nm}$. A 200-nm-thick Nb layer was evaporated on the pillar array surface, and the SC critical temperature T_C of the evaporated Nb layer was measured with a simultaneously evaporated reference sample and was 9.07 K. On the pillars covered with the Nb layer, an additional $\sim 1.5\text{-}\mu\text{m}$ -thick silver (Ag) layer was evaporated. Then, the sample is turned upside down and the Ag surface of the sample was pasted to a supporting substrate (microscope slide). Finally, the InP substrate was removed with mechanical polishing and subsequent ICP-RIE or selective chemical etching. The schematic of the prepared final structure is shown in Fig. 1(a) and the optical microscope image of the sample surface is shown in Fig. 1(b). Ag exhibits high optical reflectivity in the infrared spectral range and enhances extraction of emitted photons by the lateral reflection at the pillar-sidewall and Ag interface.¹⁷

At the Nb/InGaAs-based semiconductor interface shown in Fig. 1(c), penetration of Cooper pairs from the Nb superconductor to the normal semiconductor region is known as the proximity effect.¹⁰ Recently, the proximity effect was studied with tunneling spectroscopy in InAs/Al core-shell nanowires hosting a gate tunable tunneling barrier, and its spectra clearly showed the opening of SC gap in InAs nanowires.¹⁸ This directly demonstrated that the normal region in close proximity to a superconductor acquires SC properties by the penetration of Cooper pairs. In the present experiment, the InAs nanowire is replaced with the n -type InGaAs-based semiconductor. The penetration depth is related to the coherence length of electron Cooper pairs, and it is calculated to be $9.16 \times 10^{-4} (N_{3D})^{1/3} / T^{1/2} (\text{nm})$ with the physical parameters for InGaAs.^{14,19} N_{3D} is the electron concentration

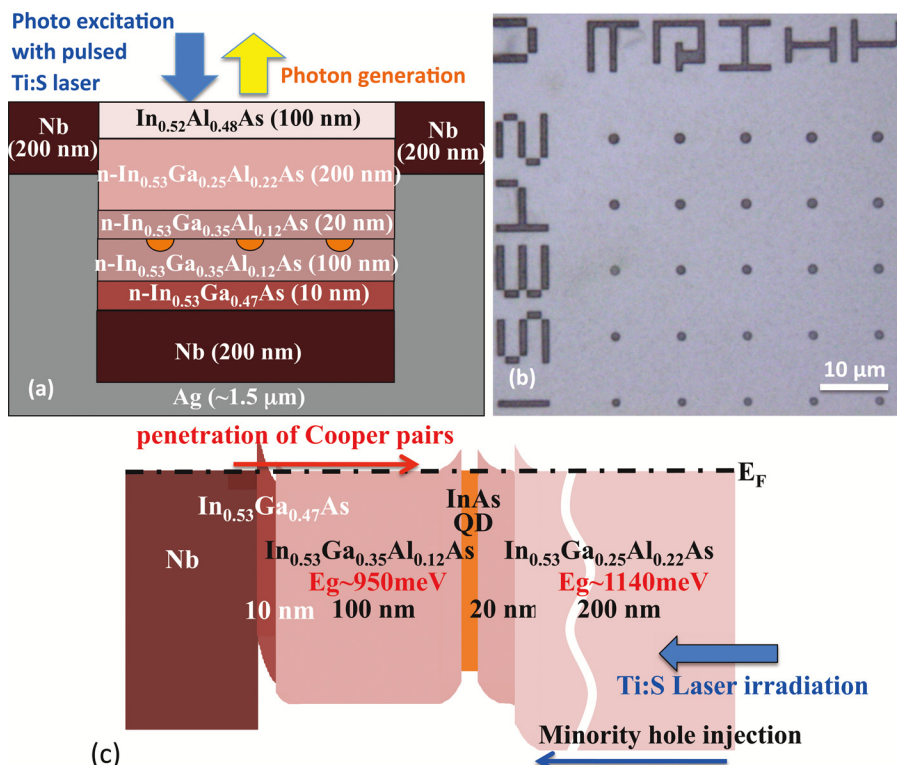


FIG. 1. (a) Schematic of Ag-embedded InAs QD heterostructure sample and the photo-excitation and photon extraction from the surface. (b) Optical microscope image of a prepared sample surface. The circles (pillars), the address numbers, and the alphabets are the surface of the embedded semiconductor and the other area is the Nb surface. (c) Schematic band structure.

in the n-type semiconductor and is $1 \times 10^{18} \text{ cm}^{-3}$. This gives the coherence length of $916/T^{1/2}(\text{nm})$ at temperature T (K) and it is $\sim 450 \text{ nm}$ at 4 K, which is much longer than the distance of 110 nm of the QD plane from the Nb/InGaAs interface.

The Schottky barrier height at the metal (Nb)/In_{0.53}Ga_{0.47}As interface is estimated to be $\sim 200 \text{ meV}$.²⁰ For Cooper pairs to penetrate into the n-type semiconductor, this barrier must be tunneled. Further barrier reduction by $\sim 50 \text{ meV}$ is estimated with the Schottky effect.²¹ Then, the depletion layer width at the interface is estimated to be $\sim 15 \text{ nm}$ for the electron concentration of $1 \times 10^{18} \text{ cm}^{-3}$ in the In_{0.53}Ga_{0.47}As layer. However, the modulation doping from the adjacent wider-bandgap n-In_{0.53}Ga_{0.35}Al_{0.12}As increases the electron concentration in the In_{0.53}Ga_{0.47}As layer and the further reduction of the depletion layer width is expected. In such a thin depletion layer, penetration of the electron wave functions into the depletion layer effectively results in residual electron concentrations in the depletion layer. Even when it is assumed to be three-orders of magnitude lower than the doping level of $1 \times 10^{18} \text{ cm}^{-3}$, the coherence length is still given as $91.6/T^{1/2}(\text{nm})$, which is much longer than the depletion layer width. Therefore, coherent tunneling of supercurrent through the Schottky barrier, which is the flow of Cooper pairs, will take place for the event of luminescence in the InAs QDs. The heterointerface barriers in the heterostructure are in the range of 90–130 meV assuming the band offset ratio of 0.7 and 0.3 for the conduction and valence bands, respectively,²² and the similar discussion on tunneling through the depletion layers at the heterointerfaces is possible. Therefore, coherent tunneling of supercurrent through InAs QDs is possible in our heterostructure samples.

III. MEASUREMENT METHOD

For luminescence measurements under pulsed excitation, the prepared sample was placed in a liquid-helium-cooled cryostat and was excited with a mode-locked pulsed Titanium:Sapphire laser (operating at the wavelength of

770 nm) with 5-ps pulse width and 76 MHz repetition rate. The laser beam was focused on one of the semiconductor pillars surface employing an objective lens (OL) with the numerical aperture (NA) of 0.4. Luminescence emitted from InAs QDs was collected with the same OL and was dispersed by a double monochromator with the 50-cm focal length and 300-grooves-per-mm gratings and was detected with a liquid-nitrogen-cooled InGaAs-photodiode array detector.

For time-resolved luminescence measurements, emission from InAs QDs was coupled into a single-mode optical fiber (SMF) with an additional OL with NA of 0.25 and was directed into a superconducting single-photon detector (SSPD) by Single Quantum BV. The laser pulse was partially converted to an electrical pulse with a p-i-n photodiode and was used as the start signal, and signal from the SSPD was used as the stop signal of a time-to-amplitude converter (TAC). To spectrally select the QD emission, a 1570-nm band-pass filter with 20-nm bandwidth was inserted in the optical path before coupling to the SMF.

IV. SPECTRAL MEASUREMENTS

Figures 2(a) and 2(b) show the excitation power dependence of QD-emission luminescence spectra measured at 4 K and 12 K, respectively, on one of the Nb/Ag embedded pillars with the diameter of $1.5 \mu\text{m}$. The excitation power is given with the time-averaged value for the pulsed excitation. The QD luminescence spectra are slightly blue shifted for the higher excitation. Although the spectra are not much temperature dependent, the luminescence intensity measured at 4 K is almost double of that at 12 K. The peak intensity measured at 4 K and 12 K and their intensity ratio are plotted against the excitation power in Fig. 2(c). The saturation behavior observed around the excitation power of $\sim 1 \mu\text{W}$ is characteristic to QDs with filling of their lowest energy states (hole filling in the present n-type heterostructure). It is clearly seen that the luminescence intensity measured at 4 K is highly enhanced by \sim two times. This substantial enhancement below the SC critical temperature of $T_C = 9.07 \text{ K}$ reproduces the

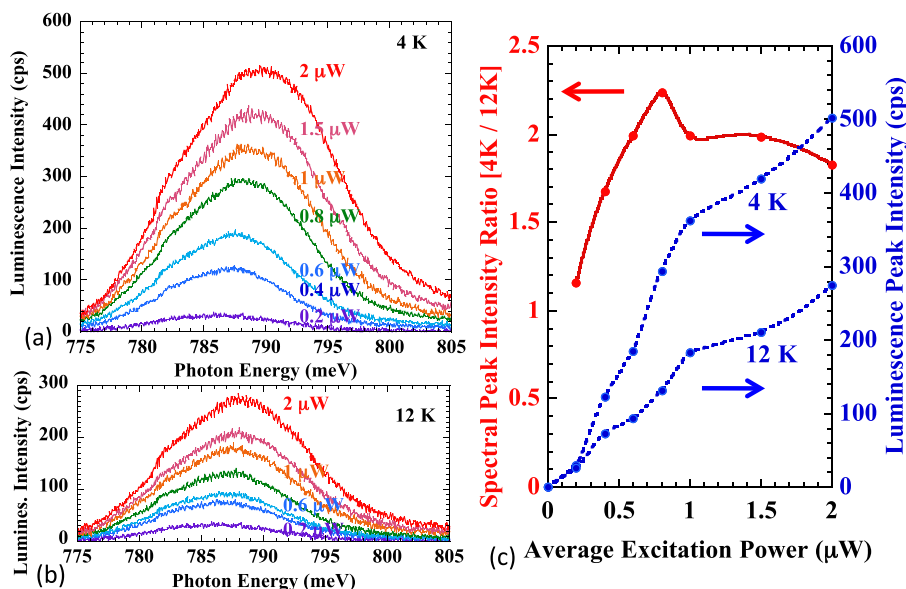


FIG. 2. (a) Excitation power dependence of time-averaged luminescence spectra measured at 4 K under pulsed excitation. Time-averaged power is given for pulsed-laser excitation ($1 \mu\text{W}$ corresponds to the pulse peak power of 2.6 mW). cps represents photon counts per second. (b) Excitation power dependence of time-averaged luminescence spectra measured at 12 K under pulsed excitation. (c) Excitation power dependence of time-averaged luminescence spectrum peak intensity at 4 K and 12 K and the ratio of 4 K to 12 K.

luminescence enhancement previously observed in QW structures.^{11,13} In what follows, we focus to time-resolved luminescence measurements to confirm the role of Cooper-pair recombination for the luminescence enhancement. For this purpose, we propose a method to identify the contribution of Cooper-pair recombination quantitatively in Sec. V.

V. ANALYTICAL METHOD

In the present n-type heterostructure, luminescence decay is regulated by the lifetime of minority holes. A lifetime generally consists of two parts: radiative lifetime τ_{rad} and non-radiative lifetime τ_{nonrad} . To distinguish the terms below and above T_C , we adopt the subscript of L and U, respectively. For temperature $T > T_C$, the lifetime is given by

$$\tau_U^{-1} = \tau_{\text{rad,U}}^{-1} + \tau_{\text{nonrad,U}}^{-1}, \quad T = T_U > T_C. \quad (1)$$

For temperature below T_C , we include the additional Cooper-pair recombination term

$$\tau_L^{-1} = \tau_{\text{rad,L}}^{-1} + \tau_{\text{nonrad,L}}^{-1} + \tau_{\text{super}}^{-1}, \quad T = T_L \leq T_C, \quad (2)$$

where τ_{super} is the SC term due to the Cooper-pair recombination. Measured luminescence intensity is proportional to the internal quantum efficiency (IQE) and is given by

$$I_{\text{Lum,U}}/I_0 = \eta_{\text{ext}}\eta_{\text{int,U}} = \frac{\tau_{\text{rad,U}}^{-1}}{\tau_{\text{nonrad,U}}^{-1} + \tau_{\text{rad,U}}^{-1}} = \frac{\tau_{\text{rad,U}}^{-1}}{\tau_U^{-1}}, \quad T = T_U > T_C, \quad (3)$$

$$I_{\text{Lum,L}}/I_0 = \eta_{\text{ext}}\eta_{\text{int,L}} = \frac{\tau_{\text{rad,L}}^{-1} + \tau_{\text{super}}^{-1}}{\tau_{\text{nonrad,L}}^{-1} + \tau_{\text{rad,L}}^{-1} + \tau_{\text{super}}^{-1}} = \frac{\tau_{\text{rad,L}}^{-1} + \tau_{\text{super}}^{-1}}{\tau_L^{-1}}, \quad T = T_L \leq T_C, \quad (4)$$

where I_{Lum} is the measured luminescence intensity and η_{int} is the IQE. η_{ext} is the external collection efficiency of photons emitted from QDs and is temperature-independent. I_0 is the luminescence intensity in the case of 100% efficiency. Normal radiative lifetime in InAs QDs remains almost constant in the low-temperature range studied in this work,²³ and we set $\tau_{\text{rad,U}}^{-1} = \tau_{\text{rad,L}}^{-1} \equiv \tau_{\text{rad}}^{-1}$. Since electrons very close to the electron Fermi level are condensed in the SC density of states (DOS) based on the Bardeen Cooper Schrieffer (BCS) theory,²⁴ this assumption is rationalized in the present highly n-type doped sample. Then taking the ratio of the luminescence intensities measured at T_L and T_U as $R_{\text{Lum}} (= I_{\text{Lum,L}}/I_{\text{Lum,U}})$, it is given by

$$R_{\text{Lum}} = \left(1 + \tau_{\text{super}}^{-1}/\tau_{\text{rad}}^{-1}\right) \frac{\tau_U^{-1}}{\tau_L^{-1}}. \quad (5)$$

Taking the ratio of the decay time constants measured at T_L and T_U as $R_{\text{lifetime}} (= \tau_U^{-1}/\tau_L^{-1})$, the ratio of the superconductive (Cooper-pair) to normal radiative recombination rates is given by

$$\tau_{\text{super}}^{-1}/\tau_{\text{rad}}^{-1} = R_{\text{Lum}}/R_{\text{lifetime}} - 1, \quad (6)$$

and it is uniquely determined with the measured values. In the total photon emission process from the QD, the numerator in the left term of Eq. (6) gives the contribution from electron Cooper pairs, and the denominator gives the one from normal electrons. From Eqs. (1)–(4), it is also possible to study the τ_{nonrad} term (nonradiative recombination), but the unique determination requests additional information how it depends on temperature.

VI. TIME-RESOLVED LUMINESCENCE MEASUREMENTS

One of the transient decay of the QD luminescence measured at 4 K and 12 K with the average excitation power of $0.8 \mu\text{W}$ is shown in Fig. 3. The measured decay is fitted by a single exponential function and the results are shown with the solid lines. The fitting results in the decay time constant τ of 3.01 ns at 4 K and 3.41 ns at 12 K.

The measured temperature dependence of the transient QD luminescence peak intensity and the luminescence decay time constant is shown in Fig. 4. The luminescence intensity shows sharp increase below T_C of 9.07 K. This well reproduces our previous observation of luminescence enhancement in SC-LEDs.^{11,13} Above T_C the decay time constant remains the same, but below T_C it shows clear decrease with temperature. This also well reproduces our previous observation of decrease of the electroluminescence decay time constant in SC-LEDs.^{14,15} These correlations of both the luminescence intensity and the decay time constant to the SC critical temperature are the clear evidence that the observed phenomenon is based on the Cooper-pair recombination in QDs penetrated from the Nb superconductor.

Employing the measured data in Fig. 4, we study the ratio of the superconductive to normal radiative recombination rates. Since both the luminescence intensity and the decay

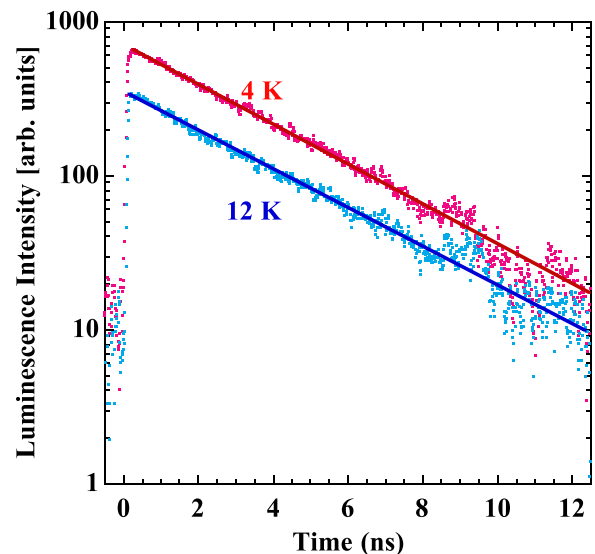


FIG. 3. Time decay of luminescence peak intensity measured at the wavelength of 1570 nm (790 meV) with the bandwidth of 20 nm (10.1 meV). The average excitation power is $0.8 \mu\text{W}$ (pulse peak power is 2.1 mW). The solid lines are the fitting curves obtained with a single exponential function.

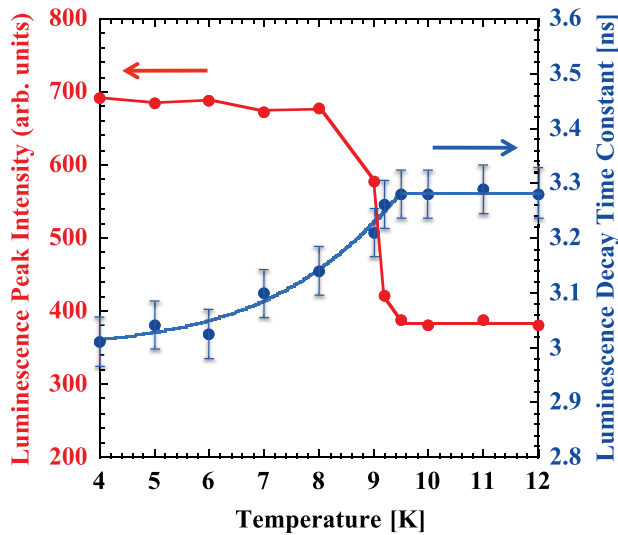


FIG. 4. Temperature dependence of transient luminescence peak intensity and luminescence decay time constant with error bars measured at an average excitation power of $0.8 \mu\text{W}$.

time constant remain almost constant above T_C in Fig. 4, the result is not much dependent on the selection of T_U above T_C in Eqs. (1)–(4), but T_U was set to the measured highest temperature of 12 K. The result is shown with closed circles in Fig. 5 and is further studied theoretically.

Our theory on the Cooper-pair luminescence presented in Ref. 12 is based on the second-order perturbation theory for electron-photon interaction, and the time-averaged expectation value of the number of emitting photon is calculated. The superconductivity effect is included through the Bogoliubov transformation from operators for electrons to those for Bogoliubov quasiparticles.²⁵ In Ref. 12, we considered two cases of finite relaxation time, which originates from scattering of electron Cooper pairs penetrated into the n-type semiconductor. One is elastic impurity scattering and the other is inelastic scatterings such as electron-phonon scattering and repulsive electron-electron scattering. Both cases resulted in similar temperature-dependent luminescence enhancement below T_C . In Fig. 5, we fitted the data with the case of elastic impurity scattering. The solid line is for $\Delta_0\tau_0/\hbar = 1.2$, where Δ_0 is half of the SC gap at zero temperature, τ_0 is the relaxation time due to elastic impurity scattering, and \hbar is the Planck constant divided by 2π . We measured T_C to be 9.07 K. However, as is shown in the inset of Fig. 5, we also find a transient temperature range and the differential resistance reaches the maximum at 9.15 K. Since T_C of intrinsic Nb is known to be 9.26 ± 0.01 K,²⁶ this transient behavior implies that SC regions survive in the Nb layer inhomogeneously in the temperature range of 9.07–9.15 K. Therefore, we set T_C as 9.15 K in the theoretical calculation. We could fit the measured superconducting Cooper-pair luminescence enhancement very nicely as shown in Fig. 5. Further discussion will be given in Sec. VII.

VII. DISCUSSION

First, we study and discuss the excitation power dependence of the transient properties shown in Fig. 3, and the

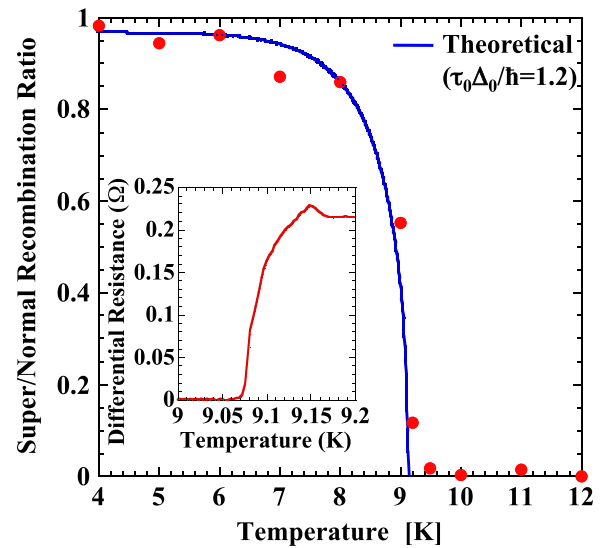


FIG. 5. Temperature dependence of the ratio of superconductive to normal radiative recombination rate. Closed circles are data from measurements. The solid line is theoretical based on Ref. 12. Δ_0 is half of the SC gap (pair potential) at zero temperature and τ_0 is the relaxation time due to elastic impurity scattering. The inset is the temperature dependence of the differential resistance measured on the evaporated Nb layer expanded near T_C . Since the theoretical calculation only deals with the superconducting recombination rate, the solid line is vertically adjusted to fit the measured overall temperature dependence.

results are summarized in Fig. 6. The measured decay time constants are shorter at 4 K in comparison to 12 K, but they show relatively weak excitation power dependence. On the other hand, the ratio of the transient luminescence peak intensities measured at 4 K and 12 K exhibits relatively sharp peak at the average excitation power of $0.8 \mu\text{W}$. Similar characteristics is observed with the time-averaged spectral-peak intensity ratio shown in Fig. 2(c). The ratios observed with the average excitation power of 1.5 and $2 \mu\text{W}$ show a different tendency between the two measurements. This is

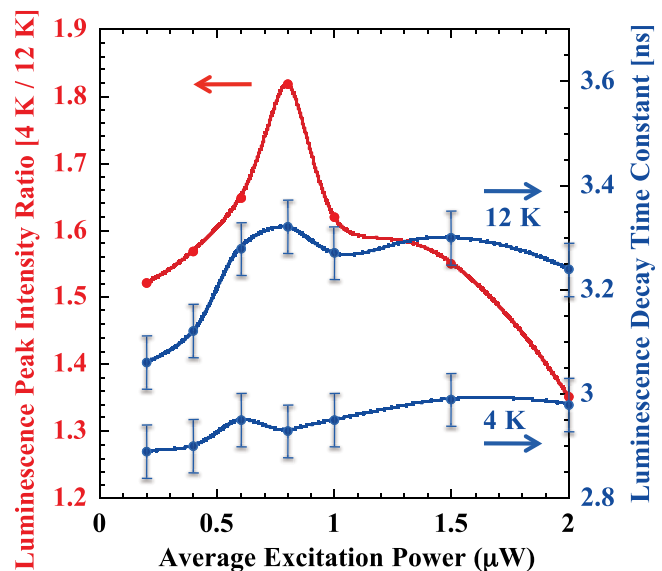


FIG. 6. Excitation power dependence of the ratio of the transient QD luminescence peak intensity at 4 K to that at 12 K (left axis) and the luminescence decay time constants with error bars at 4 K and 12 K (right axis).

related to the QD-state population saturation of photo-excited minority holes as is evident from the luminescence saturation shown in Fig. 2(c). Employing the measured data in Fig. 6, we study the ratio of the superconductive to normal radiative recombination rates with the method presented in Section V. The result is shown in Fig. 7. The ratio shows the sharp peak at the average excitation power of $0.8 \mu\text{W}$, indicating the largest enhancement of the SC Cooper-pair recombination.

In the series of samples, we observed the SC enhancement reproducibly around the photon energy of $\sim 790 \text{ meV}$ as exemplified in Fig. 2. This is because of the uniform n-type doping in the present InGaAs-based heterostructure, where the conduction-band Fermi level is almost uniform and common in the grown sample. In some high-quality samples, we observed “sharp edge” in the luminescence spectra below T_C .²⁷ We interpreted this luminescence sharp edge to reflect the sharp SC-DOS near the SC gap. Below T_C , electrons near the Fermi level form Cooper pairs and are condensed to the SC-DOS, and the SC gap opens near the electron Fermi level. Then QDs, whose conduction-band lowest energy states are near resonance with the energy of the SC-DOS, experience enhanced photon emission by the Cooper-pair recombination.^{27,28}

Concerning the excitation power dependence, the minority-hole population in the valence-band lowest QD states changes with the excitation power. When the excitation remains low, the hole population among QDs is determined mainly by the capture process of photo-generated carriers at low temperature. We presume that dominantly luminescent QDs at this stage are those of which conduction-band energy states are off resonant to the SC-DOS. With the higher excitation, population of the lowest energy states of larger dots are saturated, and the population of their excited states and carrier transfer to smaller QDs with higher QD-state energies take place through coupled excited states.²⁹ Then, when the conduction-band QD-state energies of dominantly luminescent

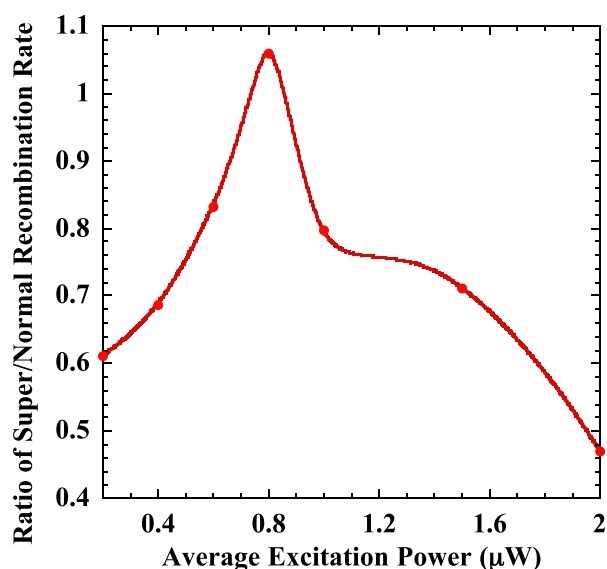


FIG. 7. Average excitation power dependence of the ratio of Cooper-pair superconductive to normal radiative recombination rates.

QDs come to near resonance with the SC-DOS, the SC recombination rate reaches the maximum as shown in Fig. 7. This results in the observed excitation power dependence with the peak excitation power of $0.8 \mu\text{W}$.

In Fig. 5, we calculated the theoretical curve numerically. In Ref. 12, we derived an analytical formula of the time-averaged expectation value of the number of emitting photon for $\Delta_0\tau_0/\hbar < 1$, i.e., for the case of higher scattering probability. The major term regulating the temperature dependence in this formula is Δ^2/T , and the enhancement is proportional to the square of half the SC gap at a given temperature T and inversely proportional to T .¹² We could fit the observed enhancement in the previous SC-LEDs with this analytical formula.^{13–15,30} The Δ^2/T dependence results in more slowly varying temperature dependence than that shown in Fig. 5 and can be approximated for $\Delta_0\tau_0/\hbar$ less than 0.2.

The parameter $\Delta_0\tau_0/\hbar \geq 1$ in Fig. 5 indicates lower scattering probability. For $\Delta_0\tau_0/\hbar < 1$ in the previous SC-LEDs, higher scattering probability prevents coherent Cooper-pair enhancement of radiative recombination. This results in the milder temperature dependence of luminescence enhancement below T_C . Therefore, we attribute the sharp increase of the luminescence enhancement below T_C to the lower scattering probability of Cooper pairs in the present sample. The difference of the samples is that the previous SC-LEDs were grown on (001) InP substrate with metalorganic chemical vapor deposition (MOCVD), while the present sample was grown on (311)B InP substrate with MBE. The other difference is that most of the previous SC-LEDs were doped n-type up to $5 \times 10^{18} \text{ cm}^{-3}$,^{11,14} while the present sample was doped $1 \times 10^{18} \text{ cm}^{-3}$. In principle, the higher electron concentration extends the coherence length as discussed in Section II, but the higher impurity concentration may increase the scattering probability.

VIII. CONCLUSIONS

We studied InAs QDs grown on an InP substrate, where electron Cooper pairs penetrate from the adjacent Nb superconductor with the proximity effect. With time-resolved measurements of luminescence around the wavelength of 1550 nm, we demonstrated abrupt luminescence enhancement and reduction of luminescence decay time constant below superconducting critical temperature. We proposed a deterministic method to find the contribution of Cooper-pair recombination and demonstrated the enhanced superconducting Cooper-pair recombination. We studied the measured temperature dependence of the Cooper-pair recombination theoretically and showed the excellent agreement with our theory. We also discussed the difference of the temperature dependence with our previously measured samples. The next issue to pursue is the demonstration of photon bunching of the emitted photons to prove the QEPP generation and the study is in progress.

ACKNOWLEDGMENTS

The authors are grateful to Professor T. Akazaki for his arrangement of our collaborative research. This work was supported in part by Nano-Macro Materials, Devices and

Systems Research Alliance and Hokkaido Innovation through NanoTechnology Support (HINTS).

- ¹P. G. Kwiat, K. Mattle, H. Weinfurter, and A. Zeilinger, *Phys. Rev. Lett.* **75**, 4337 (1995).
- ²C. K. Hong, Z. Y. Ou, and L. Mandel, *Phys. Rev. Lett.* **59**, 2044 (1987).
- ³R. Jin, R. Shimizu, I. Morohashi, K. Wakui, M. Takeoka, S. Izumi, T. Sakamoto, M. Fujiwara, T. Yamashita, S. Miki, H. Terai, Z. Wang, and M. Sasaki, *Sci. Rep.* **4**, 7468 (2014).
- ⁴D. Fattal, K. Inoue, J. Vuckovic, C. Santori, G. S. Solomon, and Y. Yamamoto, *Phys. Rev. Lett.* **92**, 037903 (2004).
- ⁵T. Kuroda, T. Mano, N. Ha, H. Nakajima, H. Kumano, B. Urbaszek, M. Jo, M. Abbarchi, Y. Sakuma, K. Sakoda, I. Suemune, X. Marie, and T. Amand, *Phys. Rev. B* **88**, 041306 (2013).
- ⁶C. L. Salter, R. M. Stevenson, I. Farrer, C. A. Nicoll, D. A. Ritchie, and A. J. Shields, *Nature* **465**, 594 (2010).
- ⁷A. J. Hudson, R. M. Stevenson, A. J. Bennett, R. J. Young, C. A. Nicoll, P. Atkinson, K. Cooper, D. A. Ritchie, and A. J. Shields, *Phys. Rev. Lett.* **99**, 266802 (2007).
- ⁸I. Suemune, T. Akazaki, K. Tanaka, M. Jo, K. Uesugi, M. Endo, H. Kumano, E. Hanamura, H. Takayanagi, M. Yamanishi, and H. Kan, *Jpn. J. Appl. Phys., Part 1* **45**, 9264 (2006).
- ⁹P. Recher, E. V. Sukhorukov, and D. Loss, *Phys. Rev. B* **63**, 165314 (2001).
- ¹⁰P. G. de Gennes, *Superconductivity of Metals and Alloys* (Boulder: Westview Press, 1999).
- ¹¹Y. Hayashi, K. Tanaka, T. Akazaki, M. Jo, H. Kumano, and I. Suemune, *Appl. Phys. Express* **1**, 011701 (2008).
- ¹²Y. Asano, I. Suemune, H. Takayanagi, and E. Hanamura, *Phys. Rev. Lett.* **103**, 187001 (2009).
- ¹³I. Suemune, Y. Hayashi, S. Kuramitsu, K. Tanaka, T. Akazaki, H. Sasakura, R. Inoue, H. Takayanagi, Y. Asano, E. Hanamura, S. Odashima, and H. Kumano, *Appl. Phys. Express* **3**, 054001 (2010).
- ¹⁴H. Sasakura, S. Kuramitsu, Y. Hayashi, K. Tanaka, T. Akazaki, E. Hanamura, R. Inoue, H. Takayanagi, Y. Asano, C. Hermannstaedter, H. Kumano, and I. Suemune, *Phys. Rev. Lett.* **107**, 157403 (2011).
- ¹⁵I. Suemune, H. Sasakura, Y. Asano, H. Kumano, R. Inoue, K. Tanaka, T. Akazaki, and H. Takayanagi, *IEICE Electron. Express* **9**, 1184 (2012).
- ¹⁶K. Akahane and N. Yamamoto, *J. Cryst. Growth* **378**, 450 (2013).
- ¹⁷H. Kumano, H. Nakajima, H. Iijima, S. Odashima, Y. Matsuo, K. Ijro, and I. Suemune, *Appl. Phys. Express* **6**, 062801 (2013).
- ¹⁸W. Chang, S. M. Albrecht, T. S. Jespersen, F. Kuemmeth, P. Krogstrup, J. Nygård, and C. M. Marcus, *Nat. Nanotechnol.* **10**, 232 (2015).
- ¹⁹T. Akazaki, T. Kawakami, and J. Nitta, *J. Appl. Phys.* **66**, 6121 (1989).
- ²⁰K. Kajiyama, Y. Mizushima, and S. Sakata, *Appl. Phys. Lett.* **23**, 458 (1973).
- ²¹S. M. Sze, *Physics of Semiconductor Devices*, 2nd ed. (Wiley, New York, 1981).
- ²²I. Vurgaftman, J. R. Meyer, and L. R. Ram-Mohan, *J. Appl. Phys.* **89**, 5815 (2001).
- ²³N. A. Jahan, C. Hermannstaedter, J.-H. Huh, H. Sasakura, T. J. Rotter, P. Ahirwar, G. Balakrishnan, K. Akahane, M. Sasaki, H. Kumano, and I. Suemune, *J. Appl. Phys.* **113**, 033506 (2013).
- ²⁴M. Tinkham, *Introduction to Superconductivity*, 2nd ed. (Dover, New York, 2004).
- ²⁵J. Unterhinninghofen, D. Manske, and A. Knorr, *Phys. Rev. B* **77**, 180509(R) (2008).
- ²⁶V. Novotny and P. P. M. Meincke, *J. Low Temp. Phys.* **18**, 147 (1975).
- ²⁷S. S. Mou, H. Irie, Y. Asano, K. Akahane, H. Kurosawa, H. Nakajima, H. Kumano, M. Sasaki, and I. Suemune, *IEEE J. Sel. Top. Quantum Electron.* **21**, 7900111 (2015).
- ²⁸S. S. Mou, H. Irie, Y. Asano, K. Akahane, H. Nakajima, H. Kumano, M. Sasaki, A. Murayama, and I. Suemune, *Phys. Rev. B* **92**, 035308 (2015).
- ²⁹C. Hermannstaedter, N. A. Jahan, J.-H. Huh, H. Sasakura, K. Akahane, M. Sasaki, and I. Suemune, *New J. Phys.* **14**, 023037 (2012).
- ³⁰I. Suemune, H. Sasakura, Y. Hayashi, K. Tanaka, T. Akazaki, Y. Asano, R. Inoue, H. Takayanagi, E. Hanamura, J.-H. Huh, C. Hermannstaedter, S. Odashima, and H. Kumano, *Jpn. J. Appl. Phys., Part 1* **51**, 010114 (2012).